Low-lying baryon resonances from lattice QCD

JOHN BULAVA[1], BÁRBARA CID-MORA[2], ANDREW D. HANLON[3], BEN HÖRZ[4], DANIEL MOHLER[5][2], COLIN MORNINGSTAR[6][*], JOSEPH MOSCOSO[7], AMY NICHOLSON[7], FERNANDO ROMERO-LÓPEZ[8], SARAH SKINNER[6], ANDRÉ WALKER-LOUD[9] (FOR THE BARYON SCATTERING (BASC) COLLABORATION)

[1] *Fakultät für Physik und Astronomie, Institut für Theoretische Physik II, Ruhr-Universität Bochum, 44780 Bochum, Germany*
[2] *GSI Helmholtz Centre for Heavy Ion Research, Darmstadt, Germany*
[3] *Physics Department, Brookhaven National Laboratory, Upton, New York 11973, USA*
[4] *Intel Deutschland GmbH, Dornacher Str. 1, 85622 Feldkirchen, Germany*
[5] *Institut für Kernphysik, Technische Universität Darmstadt, Schlossgartenstrasse 2, 64289 Darmstadt, Germany*
[6] *Dept. of Physics, Carnegie Mellon University, Pittsburgh, PA 15213, USA*
[7] *Dept. of Physics and Astronomy, U. of North Carolina, Chapel Hill, NC 27516, USA*
[8] *Center for Theor. Phys., Massachusetts Inst. of Technology, Cambridge, MA 02139, USA*
[9] *Nuclear Science Div., Lawrence Berkeley National Lab., Berkeley, CA 94720, USA*

Summary. — Recent results studying the masses and widths of low-lying baryon resonances in lattice QCD are presented. The S-wave $N\pi$ scattering lengths for both total isospins $I = 1/2$ and $I = 3/2$ are inferred from the finite-volume spectrum below the inelastic threshold together with the $I = 3/2$ P-wave containing the $\Delta(1232)$ resonance. A lattice QCD computation employing a combined basis of three-quark and meson-baryon interpolating operators with definite momentum to determine the coupled channel $\Sigma\pi$-$N\overline{K}$ scattering amplitude in the $\Lambda(1405)$ region is also presented. Our results support the picture of a two-pole structure suggested by theoretical approaches based on $SU(3)$ chiral symmetry and unitarity.

1. – Overview and Methodology

Recent results[1, 2] obtained in lattice QCD involving the scattering of nucleons and Σ baryons with pions and antikaons are presented in this talk. The goal of the studies discussed here is to determine properties of some of the low-lying baryon resonances, such as the $\Delta(1232)$ and $\Lambda(1405)$.

(*) Speaker.

arXiv:2310.08375v1 [hep-lat] 12 Oct 2023

The properties of hadron resonances are encoded in the spectrum of finite-volume stationary-state energies involving the interactions among the decay products. In lattice QCD, the finite-volume spectrum of the appropriate symmetry channels is first determined, then the scattering K-matrix is parametrized, and fits to the spectrum through the Luscher quantization condition are carried out to find best-fit values of the K-matrix parameters. With these in hand, analytic continuation is used to locate the poles of the transition matrix, which yield the resonance information.

To determine the finite-volume stationary-state spectrum in lattice QCD, a set of appropriate interpolating operators $O_i(t)$ must be introduced. The role of these operators is to create states with significant overlaps onto the low-lying stationary states through their actions on the QCD vacuum $|0\rangle$. It is important that both single-hadron and two-hadron operators are included. Using these operators, a matrix $C_{ij}(t) = \langle 0|O_i(t)O_j^\dagger(0)|0\rangle$ of temporal correlations are then evaluated. With a suitable diagonalization of this correlation matrix, the stationary-state energies can be extracted from the exponential fall-offs of the eigenvalues. The success of such extractions depends crucially on the use of very well designed operators which produce states with little overlaps onto higher lying states that contaminate the signal. Much work has been done in the past[3, 4] to design such operators. Evaluating the correlator matrix elements involving multi-hadron operators requires techniques to efficiently incorporate time-slice to time-slice quark propagators. Our computations make use of the stochastic LapH method[5].

The next step is to parametrize either the K-matrix or its inverse, then find best-fit values of these parameters by matching the spectrum obtained from the quantization condition $\det(\widetilde{K}^{-1}(E_{\rm cm}) - B^{(\boldsymbol{P})}(E_{\rm cm})) = 0$, where $E_{\rm cm}$ is the center-of-mass energy, $\widetilde{K}$ is related to K by threshold factors, and $B^{(\boldsymbol{P})}$ is the box matrix for total momentum $\boldsymbol{P}$, to the spectrum obtained from lattice QCD. The above quantization condition and the box matrix elements are discussed in detail in Ref. [6], and references contained therein.

2. – Results

The results shown here use 2000 configurations of the D200 ensemble generated by the CLS collaboration. The lattice is $64^3 \times 128$ with lattice spacing $a \sim 0.066$ fm, pion mass $m_\pi \sim 200$ MeV, and kaon mass $m_K \sim 480$ MeV.

Results for the spectrum of $N\pi$ states in finite volume are shown in Fig. 1. The scattering amplitudes obtained using this spectrum are shown in Fig. 2. The bottom left plot in this figure shows the $\Delta(1232)$ resonance. The S-wave isosinglet and isotriplet scattering lengths we obtained are

$$\text{(1)} \qquad\qquad m_\pi a_0^{3/2} = -0.2735(81) \,, \qquad m_\pi a_0^{1/2} = 0.142(22),$$

and the Δ-resonance mass and width parameters were found to be

$$\text{(2)} \qquad\qquad \frac{m_\Delta}{m_\pi} = 6.257(35), \qquad g_{\Delta,\rm BW} = 14.41(53),$$

where the Breit-Wigner parameter is given by $g_{\Delta,\rm BW}^2 q_{\rm cm}^3 \cot(\delta_{3/2^+}) = 6\pi E_{\rm cm}(m_\Delta^2 - E_{\rm cm}^2)$.

The finite-volume spectrum and resulting coupled-channel $\pi\Sigma - \bar{K}N$ transition amplitudes for the isospin $I = 0$ and strangeness $S = -1$ are shown in Fig. 3. The transition elements $t_{ij}^{(J^P)}(E_{\rm cm})$ are defined by $t^{-1} = \widetilde{K}^{-1} - i\widehat{k}$, where $\widehat{k} = \mathrm{diag}(k_{\pi\Sigma}, k_{\bar{K}N})$, with $k_{\pi\Sigma}, k_{\bar{K}N}$ defined in Ref. [2]. Another way of presenting the results for the amplitudes
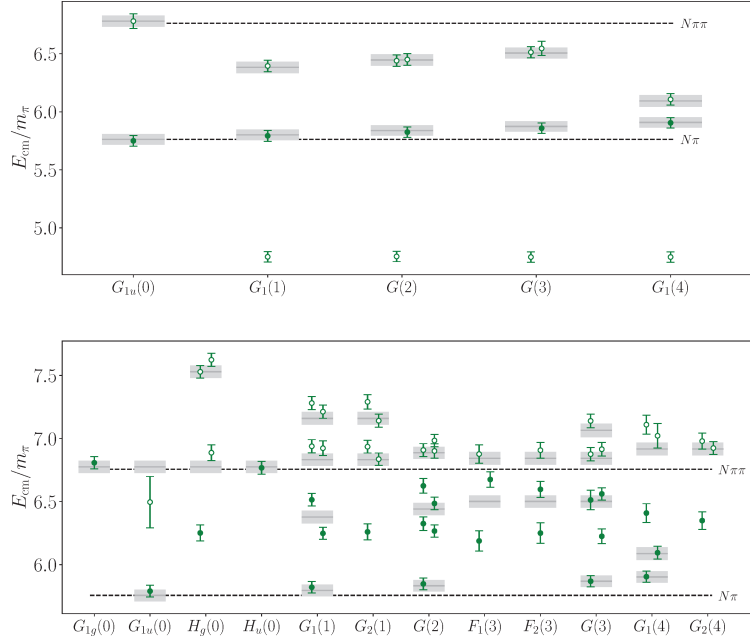
Fig. 1. – The low-lying $I = 1/2$ (top) and $I = 3/2$ (bottom) nucleon-pion spectra in the center-of-momentum frame on the D200 ensemble. Each column corresponds to a particular irrep Λ of the little group of total momentum $\boldsymbol{P}^2 = (2\pi/L)^2 \boldsymbol{d}^2$, denoted $\Lambda(\boldsymbol{d}^2)$. Dashed lines indicate the boundaries of the elastic region. Solid lines and shaded regions indicate non-interacting $N\pi$ levels and their associated statistical errors. Levels employed in subsequent fits to constrain the scattering amplitudes are shown with solid symbols. Energies are shown as ratios over the pion mass m_π.

is to show the scattering phase shifts δ_i and the inelasticity η, which are shown in the lower right plot of this figure. These amplitudes, continued to the complex energy plane, exhibit a virtual bound state below the $\Sigma\pi$ threshold and a resonance pole just below the $N\overline{K}$ threshold. These findings are broadly consistent with predictions from chiral effective field theory. The energies of these poles are

$$(3) \qquad E_1 = 1395(9)_{\text{stat}}(2)_{\text{model}}(16)_a \text{MeV},$$

$$(4) \qquad E_2 = 1456(14)_{\text{stat}}(2)_{\text{model}}(16)_a - i \times 11.7(4.3)_{\text{stat}}(4)_{\text{model}}(0.1)_a \text{MeV}.$$

The first errors are statistical, the second are from model variations, and the last from scale setting. This is a first-time calculation in lattice QCD of scattering amplitudes in a coupled-channel meson-baryon system.
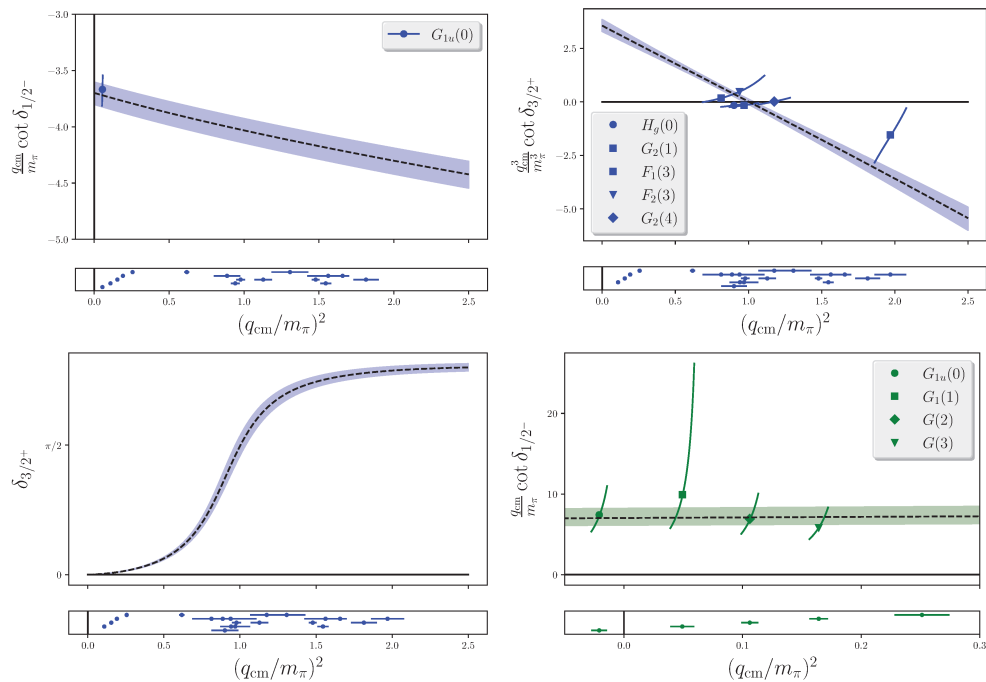
$$* \ * \ *$$

Fig. 2. – The $J^P = 1/2^-$ (top left) and $J^P = 3/2^+$ (top right) scattering amplitudes obtained from fits to the $I = 3/2$ spectrum in Fig. 1. The lower panel of each partial wave shows the squares of the center-of-mass momenta of the finite-volume levels which contribute to fitting that partial wave. Most levels, shown with solid symbols, contribute to both partial waves, so solving for the partial wave phase shift shown in the upper panel cannot be done. When a particular level couples only to the partial wave shown, a phase shift point can be obtained from the energy level and is shown in the upper panel. Hollow symbols indicate such levels. (Bottom left) Scattering phase shift of the $I = 3/2$, $J^P = 3/2^+$ partial wave containing the $\Delta(1232)$ resonance. Levels used in the fit are shown in the lower panel, but no data points are shown in the upper panel to more clearly show the final fit form. (Bottom right) Determination of the scattering length of the $J^P = 1/2^-$ wave from fits to the $I = 1/2$ spectrum in Fig. 1.

REFERENCES

[1] JOHN BULAVA et al., Nucl. Phys. B, **987** (2023) 116105.
[2] JOHN BULAVA et al., arXiv:2307.13471 [hep-lat].
[3] S. BASAK et al., Phys. Rev. D, **72** (2005) 094506.
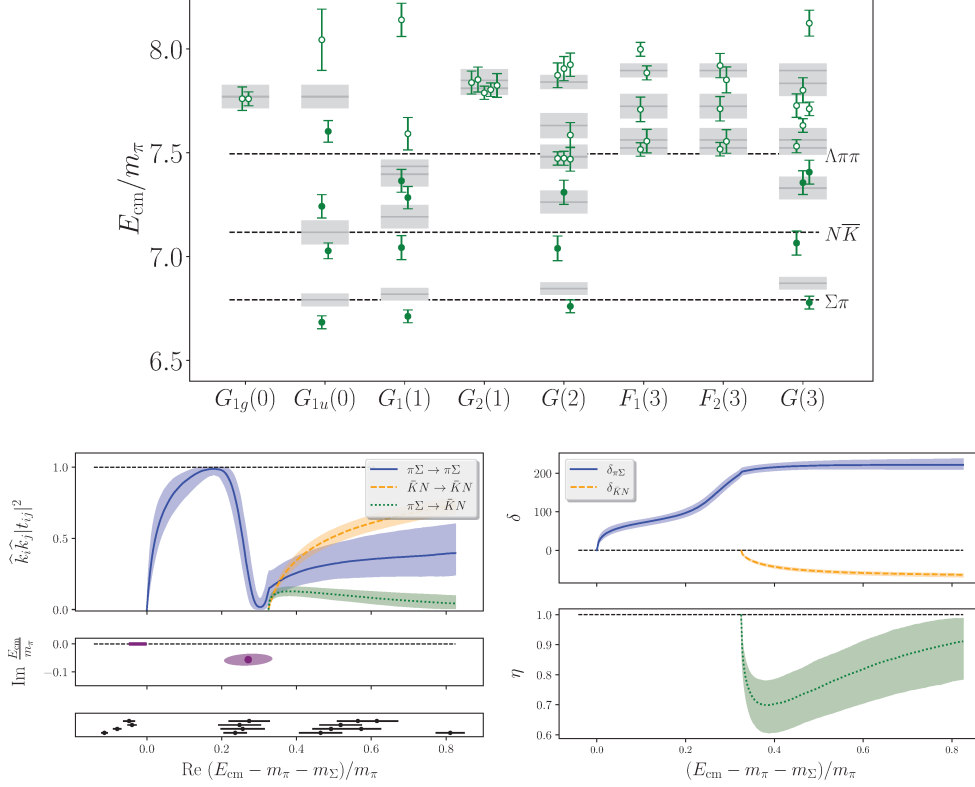[4] C. MORNINGSTAR et al., Phys. Rev. D, **88** (2013) 014511.

Fig. 3. – (Top) Finite-volume stationary-state energy spectrum, shown as green points, in the center-of-mass frame for total isospin $I = 0$, strangeness $S = -1$, and various symmetry channels indicated along the horizontal axis. The gray bands show the locations of energy sums for non-interacting two-particle combinations. Various two and three particle thresholds are shown as dashed horizontal lines. (Bottom left) The isospin $I = 0$ and strangeness $S = -1$ coupled-channel $\pi\Sigma - \bar{K}N$ transition amplitudes as a function of center-of-mass energy difference to the $\pi\Sigma$ threshold. The quantities t and $\hat{k}$ are defined in the text, and the subscripts i, j refer to the flavor channels. The middle panel shows the positions of the S-matrix poles in the complex center-of-mass energy plane on the sheets closest to the physical one. The bottom panel shows the finite-volume spectrum used to constrain the fits involving the transition amplitudes. (Bottom right) Inelasticity η and phase shifts $\delta_{\pi\Sigma}$ and $\delta_{\bar{K}N}$ against center-of-mass energy difference to the $\pi\Sigma$ threshold.

[5]   C. MORNINGSTAR *et al.*, *Phys. Rev. D*, **83** (2011) 114505.

[6]   C. MORNINGSTAR *et al.*, *Nucl. Phys. B*, **924** (2017) 477.

[7]   D. STANZIONE *et al.*, in *Proceedings of Practice and Experience in Advanced Research Computing* (PEARC '20) 2020.

[8]   CHARLES R HARRIS *et al.*, *Nature*, **585** (2020) 357.

[9]   J. D. HUNTER, *Computing in Science & Engineering*, **9** (2007) 90.

[10] R. G. EDWARDS and B. JOO, *Nucl. Phys. Proc. Suppl.*, **140** (2005) 832.